New field-emission x-ray radiography system

S. Senda, M. Tanemura, Y. Sakai, Y. Ichikawa, and S. Kita
Graduate School of Engineering, Nagoya Institute of Technology, Gokiso-cho, Showa-ku, Nagoya 466-8555, Japan

T. Otsuka
Department of Orthopaedic Surgery, Nagoya City University Medical School, 1 Kawasumi, Mizuho-cho, Mizuho-ku, Nagoya 467-8601, Japan

A. Haga and F. Okuyama[a)]
Project XR, Nagoya Institute of Technology, Gokiso-cho, Showa-ku, Nagoya 466-8555, Japan

(Received 1 April 2003; accepted 2 February 2004; published 27 April 2004)

A new field-emission x-ray radiography system based on our design is described. The key component of the system is a triode-type x-ray source with a built-in nanostructured electron source. The electron source is comprised of palladium-induced carbon nanofibers, which continue to field-emit electrons for more than 10 h at 2×10^{-7} Torr with a fluctuation of $\pm8\%$. Feedback control of the potential of the electron-extracting electrode, or the gate, reduces the current fluctuation to $\pm0.5\%$, but this current regulation does little to improve the image resolution. Our system provides sharp x-ray images of both biological and nonbiological samples. © *2004 American Institute of Physics.* [DOI: 10.1063/1.1711140]

Since the discovery of x rays,[1] x-ray radiography (XR) has played a pivotal role in medical diagnosis, as well as in the nondestructive inspection of industrial products. X-ray imaging techniques, especially of the computer-assisted type such as digital radiography,[2] have made dramatic progress over the past few decades. By contrast, the basic design of the x-ray source and the core component in XR, has undergone little change since the proposal by Coolidge in 1913,[3] i.e., thermionically emitted (TE) electrons are accelerated to bombard a metal target so as to generate x rays. Theoretically, the smaller the x-ray radiating area or the focal point, the higher the image resolution. The fine focusing of the electron beam has thus been viewed as essential to obtaining high-resolution x-ray images.[4] Unfortunately, strong focusing of TE electrons is rather difficult because of their random spatial distribution. A way to increase the image resolution in XR is to employ an electron source that can be operated in the field-emission (FE) or cold-emission[5] mode. For this, however, difficulties intrinsic to FE, in particular the short lifetimes of electron sources, must be overcome.

The FE characteristics exponentially depend on the surface-work function and the electric-field strength at the electron-emitting area,[6] the latter of which is inversely proportional to the area's radius of curvature. Due to this basic nature of FE, stable FE is premised on the unchangeability of the work function and of the dimension and/or geometry of the electron source. This requirement is fulfilled only in ultra-high vacuum (UHV), but the vast majority of electron beam tools including x-ray tubes are operated in non-UHV ambiences. In non-UHV, FE is very difficult to control, primarily because of ''cathode sputtering,'' i.e., residual gas molecules ionized through the collision with field-emitted electrons bombard the emitter and damage it.[7] A precondition for stable FE operation in non-UHV is, therefore, to develop an emitter material resistant to sputtering.

It was recently demonstrated that so-called carbon nanotubes (CNTs) are promising as the electron source in an x-ray tube.[7,8] Our previous electron sources, for example, were composed of catalytically grown CNTs, better known as ''carbon nanofibers'' (CNFs),[9] and worked for up to 80 min at 2×10^{-7} Torr, which permitted soft x-ray imaging of biological samples. However, the electron current from our emitters gradually decreased with time while fluctuating at an amplitude of $\pm10\%$, thereby limiting the emitter's lifetime to 80 min or so.[7] An intriguing fact has recently emerged, namely, that palladium (Pd)-induced CNFs ''continue'' to field-emit electrons for 10 h or longer in non-UHV with no discernible decrease in intensity. This finding prompted us to construct a compact x-ray chamber in which Pd-induced CNFs could serve as the electron source.

In brief, the procedure of producing Pd-induced CNFs was as follows. A polycrystalline tungsten (W) wire 30 μm in diameter spot-welded to stainless steel rods was placed inside a simple vacuum diode chamber at a distance of around 10 mm from a Pd disk serving as the counter electrode. A thin Pd layer was first sputter-deposited onto the W wire, followed by the CNF growth on the wire through the plasma enhanced chemical vapor deposition (CVD) process described elsewhere in detail.[10]

Figure 1(a) schematically shows the total XR system we constructed. (The design was based on our preceding work).[7] The x-ray tube, which was assembled using marketed vacuum components, is a triode in structure with the emitter assembly involving a rectangular slit as the gate (see the circle inset). The distance between the gate and the target

a)Author to whom correspondence should be addressed; electronic mail: okuyama@system.nitech.ac.jp

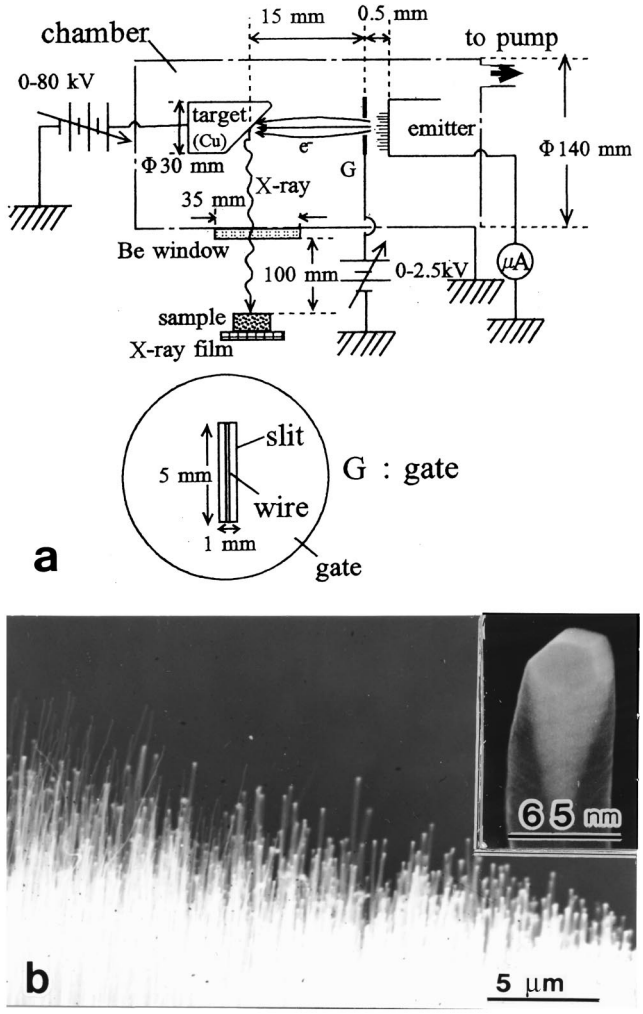

FIG. 1. (a) Diagram of the total XR system, and (b) scanning electron image of Pd-induced CNFs, with the highly magnified image of a CNF (inset). The circle in (a) shows the front view of emitter-gate assembly. The x-ray chamber is made of stainless steel.

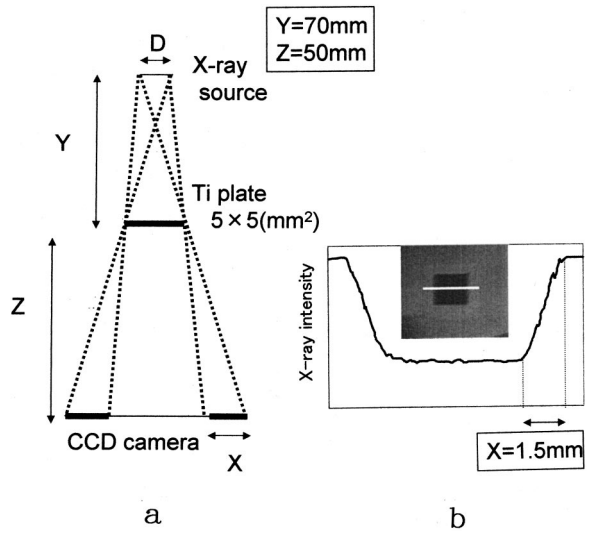

FIG. 2. Principle for estimating the focal-point dimension. (a) Two-dimensional illustration of the path of x rays passing through a rectangular titanium (Ti) plate placed just in front of the Be window. The focal-point dimension, D, is given by XY/Z, where Z denotes the location of a charge-coupled device (CCD) camera to detect x rays. (b) X-ray intensity profile along the horizontal line in the plate's image (inset), monitored on PC display. D is estimated to be around 2 mm for (b) using the respective values of X, Y, Z.

(Cu) was kept at 15 mm. When necessary, a current ''stabilizer'' consisting of a feedback circuit was linked to the gate. The x-ray tube was pumped down to 2×10^{-7} Torr with a turbo-molecular pump.

The electron source was comprised of Pd-induced CNFs described above Fig. 1(b). The CNFs were aligned on the substrate at a very high density, and were always topped with a distinctly facetted single crystal of Pd with sharp edges and points due to facet intersecting [see the inset in Fig. 1(b)]. These edges and points might serve as the electron-emission sites due to the field enhancement occurring thereon. Such emitters, henceforth referred to as ''Pd-emitters,'' worked for about 50 h in total.

The total electron current emitted from the electron source was solely governed by the potential of the gate electrode; the magnitude of the target potential had no influence on the electron emission. Typically, electrons started to be emitted at a gate potential of around 500 V, followed by a steep increase in intensity with an increase in the potential (data not shown). The actual focal spot on the target was close to a circle with a diameter of around 2 mm, independently of electron energy (Fig. 2). This fact may indicate that rough electron-beam focusing was automatically attained because the grounded tube wall deflected the obliquely emitted electrons toward the target.

Although the Pd emitters had far longer lifetimes than our previous CNF emitters, the electron currents that they emitted were not stable but fluctuated at an amplitude of $\pm8\%$ (data not shown). The current fluctuation could be reduced to $\pm0.5\%$ by using a feedback circuit, but this current stabilization had little effect on the image resolution (see later).

The practical applications of XR may be roughly classified into industrial and biological types. Typical of the former is the nondestructive inspection of electronic devices, or large-scale integrations (LSIs). Since the circuit patterns of LSIs are generally too fine to be resolved with x rays, the main role of XR in this application is to determine whether the electrical connections are perfect or not. Shown in Fig. 3(a) is the x-ray image of an LSI memory recorded at an electron energy of 40 keV. The image is so sharp as to resolve the respective lead wires {about 20 μm [Fig. 3(b)]}.

For biological samples, the x-ray energy must be lowered, preferably to the soft x-ray region. In terms of electron energy, any energy level below 10 keV corresponds to the soft x-ray region. X-ray imaging at such a low energy requires a long exposure time, and hence the electron emitter must be highly robust in non-UHV. Our Pd emitters met this demand.

Figure 4(a) shows the tail of a dead mouse imaged at 10 keV. The entire tail bone structure including the joints is clearly revealed. When the electron energy was lowered to 8 keV, the bone structure was invisible, but instead the tail hairs became recognizable [see Fig. 4(b)].

An image intensifier, if available, would have shortened the exposure time by five orders of magnitude or more, al-

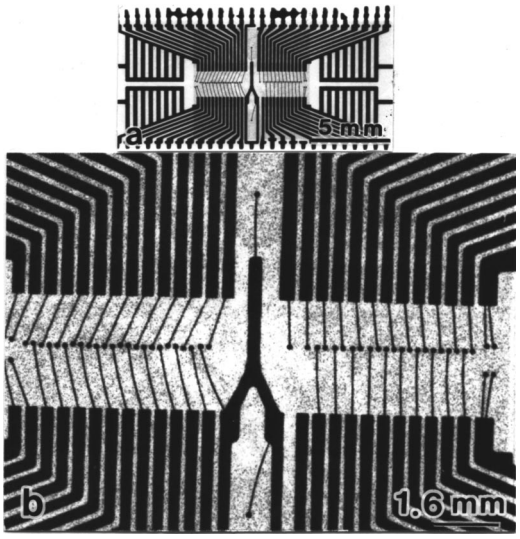

FIG. 3. (a) X-ray image of a LSI memory in the FE mode, and (b) an enlarged image of its central area. Electron energy and exposure time were 40 keV and 1 min, respectively.

lowing us to operate the x-ray source at an electron energy lower than 8 keV. Thus, FE-XR coupled with a high-resolution-image-intensifying technique would visualize living biological tissues.

Unlike TE electrons emitted in random directions, FE electrons are directed forward. This uniformity in spatial distribution of FE electrons might have been primarily responsible for producing such highly resolved x-ray images. FE electrons are also narrow in their energy spread because they are emitted from the Fermi level. A narrow energy spread of emitted electrons leads to the high resolution of electron-beam instruments, and indeed some CNTs and CNFs present sharply peaked energy distributions, promising their practical application in such instruments.[11,12] At present, however, it is unclear whether the energy uniformity of FE electrons is directly related to the resolution of x-ray images. To address this issue, energy-filtered electrons must be used to generate x rays.

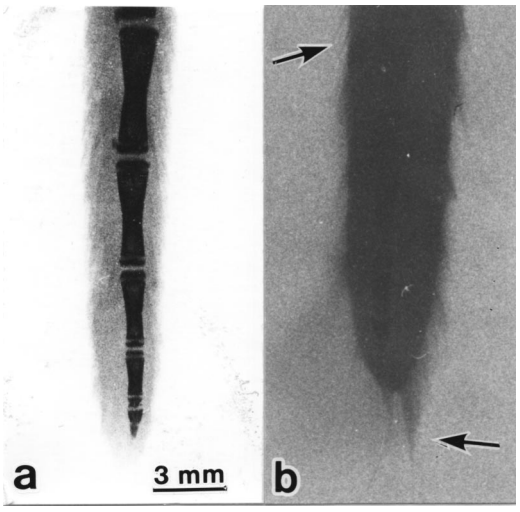

FIG. 4. (a) Tail of a dead mouse imaged at 10 keV (b) and 8 keV. Tail hairs are arrow-indicated in (b). Exposure time was (a) 30 min and (b) 15 min.

As noted earlier, the current stabilization produced no improvement in image resolution, possibly because of an integrated x-ray detection.[7] Instead, it would prolong the emitter lifetime.

The prime cause of FE emitter destruction in non-UHV is sputtering. To be more exact, a positively charged ion bombards the surface of an electron emitter to produce an atomically small protrusion thereon. Since the electric field is concentrated on such a tiny protrusion, the electron emission is dramatically enhanced from the protrusion, resulting in a meltdown of the electron emitter through excess Joule heating.[5] This means in turn, that a steep current increase generally precedes the emitter breakdown. The feedback circuit could sense the commencement of such a sudden current increase, then lowering the gate potential to stabilize the current.

The surface area of a Pd emitter contributing to electron emission was roughly estimated to be $1.5\times10^{-3}\,\mathrm{cm}^2$. The maximum electron current drawn from this effective electron-emitting area was around 1 mA, nearly equivalent to a current density of $0.7\ \mathrm{A/cm}^2$. The total electron current at this level is enough for compact XR tubes, but the emitter lifetime was limited to $\sim$30 min at this level of electron current.

This work was supported by the Ministry of Education, Culture, Sports, Science and Technology of Japan through a Grant-in-Aid for the Development of Innovative Technology No. 13201.

[1] W. C. Röntgen, Nature (London) **53**, 274 (1896).
[2] M. M. Tesic *et al.*, Digital Radiography of the Chest. Radiology **148**, 259 (1983).
[3] W. D. Coolidge, Phys. Rev. **2**, 409 (1913).
[4] A. G. Michette, *X-ray Science and Technology*, edited by A. G. Michette and C. J. Buckley (Institute of Physics, Bristol, 1993), Chap. 1.
[5] W. P. Dyke and W. W. Dolan, Adv. Electron. Electron Phys. **8**, 89 (1956).
[6] R. H. Fowler and L. W. Nordheim, Proc. R. Soc. London, Ser. A **119**, 173 (1928).
[7] H. Sugie *et al.*, Appl. Phys. Lett. **78**, 2578 (2001).
[8] G. Z. Yue *et al.*, Appl. Phys. Lett. **81**, 355 (2002).
[9] N. M. Rodriguez, J. Mater. Res. **8**, 3233 (1993).
[10] M. Tanemura *et al.*, J. Appl. Phys. **90**, 1529 (2001).
[11] M. J. Fransen, T. L. Van Rooy, and P. Kruit, Appl. Surf. Sci. **146**, 312 (1999).
[12] O. Grönig *et al.*, J. Vac. Sci. Technol. B **18**, 665 (2000).